# Role of Nuclear Quadrupole Coupling on Decoherence and Relaxation of Central Spins in Quantum Dots

N. A. Sinitsyn, Yan Li, S. A. Crooker, A. Saxena, and D. L. Smith

Phys. Rev. Lett. **109**, 166605 — Published 18 October 2012

DOI: 10.1103/PhysRevLett.109.166605

# Role of Nuclear Quadrupole Coupling on Decoherence and Relaxation of Central Spins in Quantum Dots

N. A. Sinitsyn[a], Yan Li[b], S. A. Crooker[b], A. Saxena[a], and D. L. Smith[a]
[a] *Theoretical Division, Los Alamos National Laboratory, Los Alamos, NM 87545, USA and*
[b] *National High Magnetic Field Laboratory, Los Alamos National Laboratory, Los Alamos, NM 87545, USA*
(Dated: August 3, 2012)

Strain-induced gradients of local electric fields in semiconductor quantum dots can couple to the quadrupole moments of nuclear spins. We develop a theory describing the influence of this quadrupolar coupling (QC) on the spin correlators of electron and hole "central" spins localized in such dots. We show that when the QC strength is comparable to or larger than the hyperfine coupling strength between nuclei and the central spin, the relaxation rate of the central spin is strongly enhanced and can be exponential. We demonstrate a good agreement with recent experiments on spin relaxation in hole-doped (In,Ga)As self-assembled quantum dots.

PACS numbers:

The spin of an electron or a hole in a semiconductor quantum dot is the main component of numerous proposed spintronic and quantum computing devices [1]. Spin decoherence and finite spin lifetimes are currently the major factors that limit our ability to control spin states in dots. A single "central" (*i.e.*, electron or hole) spin in a dot interacts via hyperfine coupling with a large number ($10^4-10^6$) of nuclear spins. The net effect of this coupling to the nuclear spin bath can be characterized by an effective Overhauser magnetic field $\mathbf{B_n}$ that acts upon the central spin. Within a quantum dot ensemble, each central spin precesses around a different $\mathbf{B_n}$. If $\mathbf{B_n}$ is time-independent, such precession alone cannot lead to complete relaxation of the central spin polarization. This is evidenced from the observation of spin echoes [2] that can be used to cancel the dephasing of central spins in an ensemble of dots with different constant $\mathbf{B_n}$. However, stochastic dynamics of the Overhauser field $\mathbf{B_n}$ induces irreversible relaxation of the central spin and loss of coherence [3, 4]. The physics that leads to changes of $\mathbf{B_n}$ and its corresponding influence on central spin relaxation are the subject of considerable theoretical debate [4–9].

It was suggested that, at microsecond time scales, the dynamics of the Overhauser field is dominated by hyperfine-mediated *nuclear co-flips*, which originate from unequal strengths of the hyperfine couplings of the central spin to different nuclear spins inside the same dot [4]. Numerical simulations by Al-Hassanieh et al. [9] showed that such co-flips generally lead only to a logarithmically slow central spin relaxation. In contrast, recent experimental studies with hole-doped (In,Ga)As quantum dots reported a nearly ideal Lorentzian shape of the spin noise power spectrum, indicating exponential relaxation of central hole spins rather than a power-law or logarithmic relaxation [10].

Here we show that quadrupolar couplings (QC) of nuclear spins to the strain induced electric field gradients inside typical semiconductor quantum dots can induce relatively fast dynamics of the Overhauser field $\mathbf{B_n}$, and consequently accelerated relaxation of electron and hole spins in weak external fields. Our model directly applies to InGaAs self-assembled quantum dot systems, which are among the most popular platforms for spin memories and qubits [11, 12]; however, the model applies generally to all dots composed of quadrupolar-active nuclei. We model such a nuclear spin bath by introducing static fields acting on nuclear spins due to QC, in addition to the hyperfine couplings to the central spin. We numerically compute the dynamics of our model by applying a time-dependent mean field (TDMF) algorithm [9] that allows us to study the relaxation of a central spin coupled to an unpolarized spin bath containing up to ten thousand nuclear spins.

At low temperatures and at time scales shorter than a millisecond, a Hamiltonian that captures central spin dynamics in quantum dots has the following form:

$$\hat{H} = \sum_{i=1}^{N}\left(\gamma_{||}^{i}\hat{I}_{iz}\hat{S}_z + \gamma_{\perp}^{i}(\hat{I}_{ix}\hat{S}_x + \hat{I}_{iy}\hat{S}_y)\right) + g_z B_z \hat{S}_z + g_x B_x \hat{S}_x + g_y B_y \hat{S}_y + \sum_{i=1}^{N}\frac{\gamma_Q^i}{2}\left((\hat{\boldsymbol{I}}_i\cdot\boldsymbol{n}_i)^2 - \frac{I(I+1)}{3}\right), \quad (1)$$

where $\hat{S}$ and $\hat{I}_i$ stand for spin operators of, respectively, central and nuclear spins; $B_\alpha$ is an applied magnetic field component along the axis $\alpha$; $g_\alpha$ is the corresponding component of the central spin g-factor. Index $i$ runs though all nuclear spins that interact with the central spin. Parameters $\gamma_{||}^i$ and $\gamma_\perp^i$ are the out-of-plane (longitudinal) and in-plane (transverse) coupling strengths, respectively, between the central spin and $i$-th nuclear spin. Henceforth we drop index $i$ for coupling strengths when we discuss their typical magnitudes. For electrons, $\gamma_{||}$ and $\gamma_\perp$ have similar magnitudes, but $\gamma_{||}$ and $\gamma_\perp$ are quite different for holes. For the latter case, the ratio of transverse to out-of-plane couplings, $\beta = \gamma_\perp/\gamma_{||}$ varies in different samples in the range [10, 13] $\beta \sim 0.1-0.7$. Additional coupling terms in the Hamiltonian such as $\sim \hat{S}_z\hat{I}_{ix}$

are allowed but they were estimated to be negligibly small both in electron and in hole-doped dots [13], and we will disregard them. We also disregard the Zeeman coupling between the external field and nuclear spins because we consider only weak external fields, about the size of the Overhauser field ($\sim 25$ Gauss for an InGaAs hole doped dot [10]).

The last term in (1) describes QC with characteristic strength $\gamma_Q^i$, and coupling anisotropy vector $\boldsymbol{n}_i$ for the $i$-th nuclear spin. QC is allowed for nuclei having spin larger than 1/2. QC has previously proved important in experiments on polarized spin bath relaxation in GaAs [14–18]; however, it has been generally disregarded in the context of central spin relaxation with initially unpolarized nuclear spin baths, both in electron [5, 6, 9] and in hole-doped [13] dots. We believe that this omission cannot be justified except in certain materials, such as Si, that contain predominantly spin-0 or spin-1/2 nuclei. In the widely studied InGaAs dot system, the most abundant indium isotopes $^{115}$In and $^{113}$In have $I = 9/2$, and Ga and As isotopes have $I = 3/2$. According to many studies [14, 15, 19], $\gamma_Q \sim 2 - 4$ MHz for indium atoms in GaAs at a typical strain of 3-4% inside a dot, which translates for spin 9/2 into a characteristic level splitting $\gamma_c \equiv \gamma_Q|\boldsymbol{I}| \sim 10$ MHz. This value is at least an order of magnitude larger than the effective hyperfine coupling $\gamma_{||} \sim 0.1$-$0.5$ MHz in a typical hole-doped quantum dot with $N \sim 10^5$ nuclei [13, 20]. Recent NMR studies of InGaAs dots also showed that the directions of QC anisotropy axes $\boldsymbol{n}_i$ are strongly non-uniform inside a dot and do not align with the sample growth anisotropy [19]. To include this fact, we will assume that the local anisotropy vector $\boldsymbol{n}_i$ for the $i$-th nuclear spin points in a random direction, which is chosen independently for each nuclear spin. Note that this does not exclude arbitrary spatial correlations of different $\boldsymbol{n}_i$ inside the dot.

The Hamiltonian (1) belongs to the class of spin bath models, in which noncollinear static fields act on nuclear spins independently of the coupling to the central spin. In order to compare different models of this class, we introduce a parameter $\gamma_c$ that characterizes the typical energy level splitting of nuclear spins by static fields. Our theory shows that this parameter determines all the essential effects of the static fields irrespective of the details of the interactions. This renders our theory applicable to spin baths with different sizes of nuclear spins $I$. Our results extend beyond the Hamiltonian (1). In fact, the *minimal model* of our class of spin baths can be formulated in terms of the central spin problem with only a nuclear spin-1/2 Hamiltonian:

$$\hat{H} = \boldsymbol{B}\cdot\hat{\boldsymbol{\sigma}} + \sum_{i=1}^{N}[\gamma_{||}^i\hat{\sigma}_z\hat{\sigma}_z^i + \\ + \gamma_{\perp}^i(\hat{\sigma}_x\hat{\sigma}_x^i + \hat{\sigma}_y\hat{\sigma}_y^i) + \gamma_c^i(\hat{\boldsymbol{\sigma}}^i\cdot\boldsymbol{n}^i)], \qquad (2)$$

where the last term mimics the effect of QC, $\hat{\boldsymbol{\sigma}}$ is the Pauli operator of the central (electron or hole) spin, $\hat{\sigma}_\alpha^i$ is the $\alpha$-component of the Pauli operator for the $i$-th nuclear spin, and $\gamma_c^i$ corresponds to the size of the characteristic level splitting for the $i$-th nuclear spin with quantization axis $\boldsymbol{n}^i$.

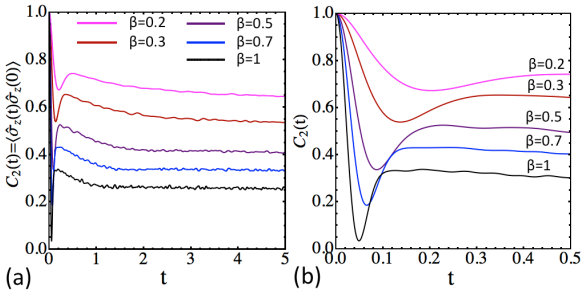


FIG. 1: Spin correlator $C_2(t) = \langle\hat{\sigma}_z(t)\hat{\sigma}_z(0)\rangle$ at $\gamma_c = 0$, $\gamma_{||} \equiv \langle\gamma_{||}\rangle = 1$, $N = 700$ nuclear spins, and $\boldsymbol{B} = 0$, shown up to times (a) $t = 5/\gamma_{||}$ and (b) $t = 0.5/\gamma_{||}$ (time $t$ is in units of $1/\gamma_{||}$). Here $\beta = \gamma_\perp/\gamma_{||}$ is the hyperfine coupling anisotropy.

We will compare, in Fig. 2, the dynamics of the model with the Hamiltonian (1) for the spin bath with $I = 1$ and the minimal model (2) at the same characteristic value of $\gamma_c$. Results are almost indistinguishable, so in the rest of the main text, we will show numerical results only for the minimal model to illustrate all the effects.

In the supplementary file [21], we describe the TDMF approach and provide additional numerical tests for evolution with $N$ from 250 to 10000 nuclear spins, the Hamiltonian (1) with $I = 1$, and the classical limit $I \gg 1$, which are all found to be in vey good agreement with the theory that we develop here.

We present our results for central spin temporal correlators that were obtained for the model (2) with $N = 700$ spin-1/2 nuclei at equilibrium. Before each simulation, we chose $\gamma_{||}^i = 2\gamma_{||}*r_{1i}$, $\gamma_\perp^i = 2\beta\gamma_{||}*r_{2i}$ and $\gamma_c^i = 2\gamma_c*r_{3i}$, where $r_{1i}$, $r_{2i}$ and $r_{3i}$ are random numbers from a uniform distribution in the interval $(0, 1)$. We set the energy scale so that $\gamma_{||} = 1$. Note that we chose widths of parameter distributions to be comparable to the mean values as suggested in [9]. Vectors $\boldsymbol{n}^i$ point in random directions and the time step was $dt = 0.0001$. Averaging was performed over 1000 and over 30000 randomly chosen initial state vectors (both for central and nuclear spins) for the calculation of, respectively, noise power and real-time correlators.

In Fig. 1(a) we show our numerical results for the central spin correlator, $C_2(t) = \langle\hat{\sigma}_z(t)\hat{\sigma}_z(0)\rangle$, obtained from the evolution of the Hamiltonian (2) in the absence of quadrupolar interactions ($\gamma_c = 0$). Different curves correspond to different values of the coupling anisotropy $\beta$. All curves start at $C_2(0) = 1$. Figure 1(b) resolves the part of Fig. 1(a) with $t < 0.5$. The appearance and shape of the deep local minimum of $C_2(t)$ in Fig. 1(b) is well understood [4, 13] as being due to dephasing caused by

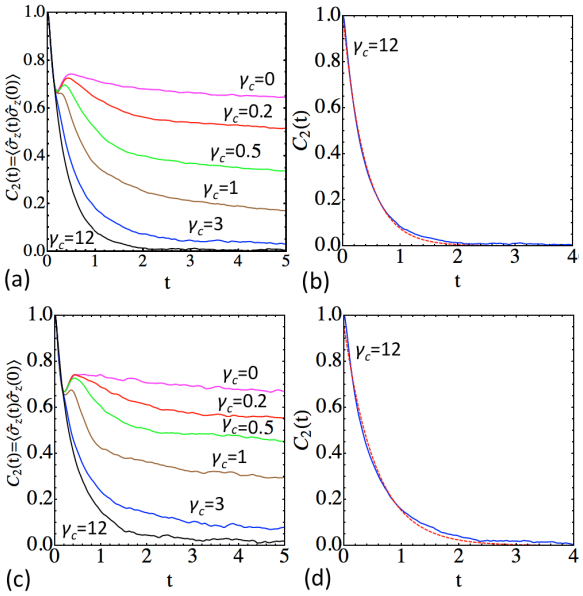


FIG. 2: (a) The real time central spin-spin correlator for different magnitudes of the static field $\gamma_c$ in spin-1/2 bath. (b) Exponential fit (dashed red) of the spin correlator (blue) for spin-1/2 bath at $\gamma_c = 12$ in units of $\gamma_{||}$. (c) Central spin correlator in spin bath with $I = 1$ and quadrupole coupling $\gamma_Q^i = 4\gamma_c^i$. (d) Exponential fit (dashed red) of spin correlator in spin-1 bath at $\gamma_c = 12$. In all cases: $\beta = 0.2$ and $\boldsymbol{B} = 0$.

ensemble central spin precession around the Overhauser fields $\mathbf{B_n} = \sum_{i=1}^{N}[\gamma_\perp^i\langle\hat\sigma_x^i\rangle\mathbf{x} + \gamma_\perp^i\langle\hat\sigma_y^i\rangle\mathbf{y} + \gamma_{||}^i\langle\hat\sigma_z^i\rangle\mathbf{z}]$. Figure 1(a) shows that a fraction of the central spin polarization additionally relaxes during a longer time interval that is of order $1/\langle\gamma_{||}\rangle$. This relaxation follows from the co-flip effect [5, 6, 9]. Figure. 1(a) confirms previous observation [9], which was made for the case $\beta = 1$, that only a fraction of the central spin polarization relaxes via this mechanism on time scales of interest. It also shows that the correlator decay is strongly suppressed by hyperfine coupling anisotropy. This means that standard co-flip effect cannot explain the observed spin relaxation at a fraction of a microsecond in experiments with hole-doped dots [10, 11, 22], for which $1/\langle\gamma_{||}\rangle$ corresponds to several microseconds [13].

Figure 2 shows the central spin correlator $C_2(t)$ for several different mean values of QC [as tuned by the static field $\gamma_c$ to compare spin-1/2 bath in Figs. 2(a-b) and spin-1 bath with $\gamma_Q^i = 4\gamma_c^i$ in Figs. 2(c-d)] at strong anisotropy $\beta = 0.2$. The effect of $\gamma_c \neq 0$ is considerable. Even at $\gamma_c = 0.2 < \langle\gamma_{||}\rangle$, relaxation of the central spin is already much faster than at $\gamma_c = 0$. For $\gamma_c > \gamma_{||}$, we find qualitative changes: the local minimum disappears, relaxation becomes almost complete and furthermore becomes exponential [see Fig. 2(b)]. At $\gamma_c > 8$, the exponential relaxation rate saturates at a value that does not depend on $\gamma_c$ any longer. Figures 2(c-d) show analogous results for the nuclear spin bath with the Hamiltoninan (1) and

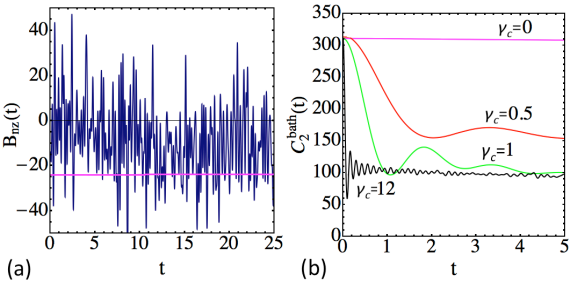


FIG. 3: For $\beta = 0.2$: (a) Typical Overhauser field dynamics for $\gamma_c = 0$ (pink line) and $\gamma_c = 8$ (blue). (b) Real time Overhauser field correlator $C_2^{\rm bath}(t) = \langle B_{nz}(t)B_{nz}(0)\rangle$.

$I = 1$ with $\gamma_Q^i = 4\gamma_c^i$, which corresponds to the same characteristic splitting of energy levels by QC. It shows that by changing the size of spins and form of the coupling but keeping the same characteristic $\gamma_c$, the form of the central spin correlator does not change.

To better understand this change of behavior, it is instructive to look at the dynamics of $B_{nz}$, the Overhauser field component along the $z$-axis. Figure 3 shows examples of $B_{nz}(t)$ starting from a random initial condition for all spins. When $\gamma_c = 0$, $B_{nz}$ is practically frozen. However, for $\gamma_c > \gamma_{||}$ values, $B_{nz}$ quickly fluctuates with the amplitude of the typical Overhauser field strength. Figure 3(b) shows that in the latter case, the bath spin correlator $C_2^{\rm bath}(t) = \langle B_{nz}(t)B_{nz}(0)\rangle$ decays during $t < 1/\gamma_c$ to a smaller but nonzero value. For $\gamma_c \gg \gamma_{||}$, nuclear spins simply precess around their local static fields from the QC. Fluctuations that are seen in Fig. 3(a) are then merely due to the difference of precession frequencies and precession axis directions for different nuclear spins in one dot. In contrast, when $\gamma_c/\gamma_{||} < 1$, nuclear spin precessions are synchronized by a stronger hyperfine coupling that suppresses fluctuations of $B_{nz}$.

When $\gamma_c > \gamma_{||}$, there can be two distinct regimes of central spin polarization dynamics. The first regime appears when fluctuations of the Overhauser field are so fast that the adiabaticity conditions break down and the central spin polarization cannot follow the direction of the Overhauser field. This most likely can happen when $B_{nz}$ passes through zero values and the Landau-Zener transition probability, $p_{LZ} = 1 - \exp(-\pi(B_{n\perp})^2/v)$ is substantially different from unity. Here $v = (dB_{nz}/dt)_{B_{nz}=0}$ and $B_{n\perp} \sim \gamma_\perp\sqrt{N}$ is the typical value of the Overhauser field transverse to the $z$-axis direction. In this case, each time $B_{nz}$ changes sign, the central spin has substantial probability of not following the Overhauser field so that its dynamics become stochastic with exponential relaxation of the central spin correlator [23]. To estimate $p_{LZ}$ we note that, according to Fig. 3(b), when $\gamma_c > \gamma_{||}$, the time $1/\gamma_c$ sets the scale for the correlator decay time of the Overhauser field. The latter changes during this time by the amount $\delta B_{nz} \sim \gamma_{||}\sqrt{N}$. Hence, the rate of change

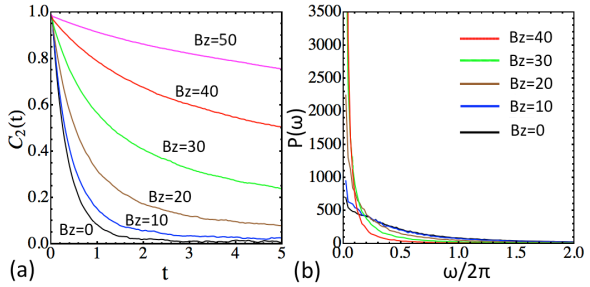


FIG. 4: (a) Real time spin correlator and (b) frequency power spectrum $P(\omega) = \int dt e^{i\omega t} \langle \hat{\sigma}_z(t)\hat{\sigma}_z(0)\rangle$ for different values of external out-of-plane magnetic field $B_z$; $\gamma_c = 8$, and $\beta = 0.2$.

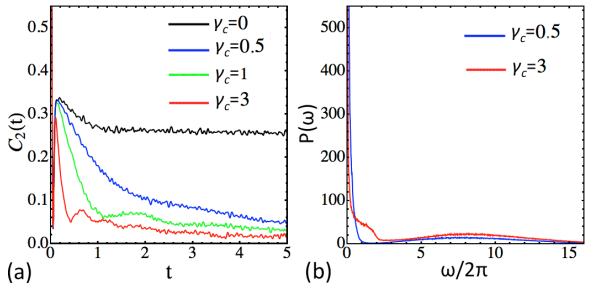


FIG. 5: Central spin correlator at $\beta = 1$ in zero external field: (a) Real time correlator and (b) frequency power spectrum.

of the Overhauser field is $v \sim \gamma_{||}\sqrt{N}\gamma_c$, and exponential relaxation can occur when two conditions are satisfied:

$$\gamma_c > \gamma_{||}, \quad \text{and} \quad \eta \equiv \beta^2\gamma_{||}\sqrt{N}/\gamma_c < 1. \tag{3}$$

For our numerical test with $N = 700$ and $\beta = 0.2$, we find that (3) is satisfied when $\gamma_c/\gamma_{||} \sim 1$. This result is in agreement with Fig. 2. The exponential relaxation time, $\tau_{\rm rel}$, roughly corresponds to the value of $1/\gamma_c$ at which $p_{LZ} \sim 1/2$, i.e. $\tau_{\rm rel} \sim 1/[\beta^2\gamma_{||}\sqrt{N}]$. For the hole-doped dots [10, 22], we assume $N = 10^5$, $\beta = 0.2$, $\gamma_c/\gamma_{||} = 25$, which gives $\eta = 0.4 < 1$, *i.e.* it agrees with the observed Lorentzian shape of the hole spin noise power spectrum in [10]. Considering that $1/\gamma_{||}$ corresponds to several microseconds in hole-doped dots, we find the relaxation time to be a fraction of a microsecond, which also agrees with the experimentally measured value $\tau_{\rm rel} \sim 0.4\ \mu$s at a zero external field [10]. Our model is also in good agreement with other experimental observations: For example, when an external out-of-plane magnetic field was applied, the central spin relaxation was suppressed [10, 11] when this field exceeded $\gamma_{||}\sqrt{N}$. In Fig. 4(a) we confirm this fact numerically. Figure 4(b) also shows our numerical results for the effect of an applied magnetic field on the hole spin noise power spectrum, $P(\omega) = \int dt e^{i\omega t}\langle \hat{\sigma}_z(t)\hat{\sigma}_z(0)\rangle$, which is in good agreement with experimental measurements of this spectrum in external fields [10, 11].

The second regime corresponds to the case when fluctuations of the Overhauser field are strong but the central spin follows the direction of the Overhauser field adiabatically. This happens when

$$\gamma_c > \gamma_{||}, \quad \eta > 1. \tag{4}$$

For *electron-doped* InGaAs dots, condition (4) would likely be satisfied because of a lack of anisotropy ($\beta = 1$). Assuming that such a dot has $N \sim 10^5$ nuclei and $\gamma_c/\gamma_{||} = 3$, we find $\eta \sim 10^2 \gg 1$, *i.e.* the central spin dynamics is well within the adiabatic regime. For such conditions, the central correlator has to follow the correlation pattern of the Overhauser field, as in Fig. 3(b).

Figure 5(a) shows our results for the real time correlator for $\beta = 1$ (electron-doped dots) and $N = 700$. The case $\gamma_c = 3$ corresponds to conditions (4). The first minimum of $C_2(t)$ in Fig. 5(a) is due to dephasing effects. Note that it is not destroyed by Overhauser field fluctuations, unlike the case with $\beta = 0.2$. At longer times, $C_2(t)$ qualitatively follows the Overhauser field correlation pattern, *i.e.* it decays to a small but non-zero value during a time $\sim 1/\gamma_c$, followed by a long relaxation tail. Figure 5(b) shows that a specific feature of the regime (4), which distinguishes it from the case with $\gamma_c < \gamma_{||}$, is the appearance of a shoulder in the low frequency peak of the spin noise. An additional feature of the power spectrum at $\eta > 1$ is the presence of a second broad small amplitude Gaussian peak at high frequencies.

*In conclusion,* we identified three regimes with distinct central spin dynamics in the presence of QC at low temperatures and weak external fields: (i) the regime of exponential relaxation of the spin correlator, which is defined by Eq. (3); (ii) the regime with the central spin following Overhauser field adiabatically, which is defined by Eq. (4); and (iii) the regime of weak QC, $0 < \gamma_c < \gamma_{||}$, which is qualitatively similar to $\gamma_c = 0$. We showed that hole-doped InGaAs dots [10] likely correspond to the exponential relaxation regime and that electron-doped dots correspond to the regime (ii). Regime (iii) is potentially applicable to electrostatically defined dots with a nearly perfect atomic lattice.


[1] R.-B. Liu, W. Yao, and L. J. Sham, Adv. Phys. **59**, 703 (2010); I. Zutic, J. Fabian, and S. Das Sarma, Rev. Mod. Phys. **76**, 323 (2004); R. Hanson, L. P. Kouwenhoven, J. R. Petta, S. Tarucha, and L. M. K. Vandersypen, Rev. Mod. Phys. **79**, 1217 (2007); D. Loss, and D.P. DiVincenzo, Phys. Rev. A **57**, 120 (1998).

[2] J. R. Petta *et al.*, Science **309**, 2180 (2005); F. H. L. Koppens, K. C. Nowack, and L. M. K. Vandersypen, Phys. Rev. Lett. **100**, 236802 (2008).

[3] O. Tsyplyatyev and D. Loss, Phys. Rev. Lett. **106**, 106803 (2011); L. Cywinski, V. V. Dobrovitski, and S. Das Sarma, Phys. Rev. B **82**, 035315 (2010).

[4] I. A. Merkulov, Al. L. Efros, and M. Rosen, Phys. Rev. B **65**, 205309 (2002).

[5] J. Fischer, W. A. Coish, D. V. Bulaev, and D. Loss, Phys. Rev. B **78**, 155329 (2008).

[6] A. Khaetskii, D. Loss, and L. Glazman, Phys. Rev. B **67**, 195329 (2003).

[7] S. Lee, J. Appl. Phys. **97**, 043706 (2005).

[8] Sigurdur I. Erlingsson and Yuli V. Nazarov Phys. Rev. B **70**, 205327 (2004).

[9] K. A. Al-Hassanieh, V. V. Dobrovitski, E. Dagotto, and B. N. Harmon, Phys. Rev. Lett. **97**, 037204 (2006).

[10] Yan Li, *et al.*, Phys. Rev. Lett. **108**, 186603 (2012).

[11] R. Dahbashi, *et al.*, Appl. Phys. Lett. **100**, 031906 (2012).

[12] A. C. Johnson, *et al.*, Nature **435**, 925 (2005); J. L. Robb, *et al.*, Appl. Phys. Lett. **90**, 153118 (2007); D. Heiss, *et al.*, Phys. Rev. B **82**, 245316 (2010); M. Paillard, *et al.*, Phys. Rev. Lett. **86**, 1634 (2001); D. Heiss *et al.*, Phys. Rev. B **76**, 241306 (2007); P. Asshoff, *et al.*, J. Phys.: Conf. Ser. **200**, 062002 (2010); X. Xu, *et al.*, Phys. Rev. Lett. **99**, 097401 (2007); U. Zameer, *et al.,* Proc. SPIE, 827211 (2012); P.-F. Braun, *et al.*, Braz. J. Phys. **36**, 482 (2006); P.-F. Braun, *et al.*, Phys. Rev. Lett. **94**, 116601 (2005); B. Eble, *et al.*, Phys. Rev. Lett. **102**, 146601 (2009).

[13] C. Testelin, F. Bernardot, B. Eble, and M. Chamarro, *Phys. Rev. B* **79**, 195440 (2009).

[14] R. I. Dzhioev and V. L. Korenev, Phys. Rev. Lett. **99**, 037401 (2007).

[15] P. Maletinsky, M. Kroner, and A. Imamoglu, Nature Physics **5**, 407 (2009).

[16] K. Flisinski *et al.*, Phys. Rev. B **82**, 081308 (2010).

[17] J. Ishihara *et al.*, Jpn. J. Appl. Phys. **50**, 04DM03 (2011).

[18] C-W. Huang, and X. Hu, Phys. Rev. B **81**, 205304 (2010).

[19] C. Bulutay, Phys. Rev. B **85**, 115313 (2012).

[20] M. Yu. Petrov *et al.*, Phys. Rev. B **78**, 045315 (2008).

[21] Supplementary Material.

[22] F. Fras, *et al.*, Phys. Rev. B **84**, 125431 (2011).

[23] N.V. Prokof'ev and P.C.E. Stamp, Rep. Prog. Phys. **63**, 669 (2000); N. A. Sinitsyn and V. V. Dobrovitski, Phys. Rev. B **70**, 174449, (2004); N. A. Sinitsyn and N. Prokof'ev, Phys. Rev. B **67**, 134403, (2003).